Journal of Solid State Electrochemistry (2023) 27:1477–1492
https://doi.org/10.1007/s10008-023-05446-5

ORIGINAL PAPER

Self-healable Nafion-poly(vinyl alcohol)/phosphotungstic acid proton exchange membrane prepared by freezing–thawing method for direct methanol fuel cell

Wei Wuen Ng[1] · Hui San Thiam[1,2] · Yean Ling Pang[1,2] · Yun Seng Lim[1] · Jianhui Wong[1]

Received: 11 December 2022 / Revised: 4 February 2023 / Accepted: 25 February 2023 / Published online: 4 March 2023

Abstract

Getting the direct methanol fuel cell (DMFC) closer to mass production requires the creation of a high-performance and long-lasting proton exchange membrane (PEM). In this study, self-healable PEMs, Nafion-poly(vinyl alcohol)/phosphotungstic acid (N-PVA/HPW), were prepared through a simple freezing–thawing method. HPW acted as proton conductors, while PVA with reversible hydrogen bonds contributed to the self-repair ability of the membrane. The proton conductivity of the N-PVA/HPW membranes was found to be comparable to that of the pristine Nafion membrane owing to the additional proton-conducting sites and improved water retention provided by the HPW. Along with this, the packed structure of the mixed-matrix membranes led to a lower methanol permeability in all the N-PVA/HPW membranes compared to recast Nafion. As a result, N-PVA/HPW20 membrane with acceptable proton conductivity (0.062 S cm^{-1}) and reduced methanol permeability (2.75×10^{-6} cm^2 s^{-1}) achieved the highest selectivity, where selectivity is a well-known indicator of a membrane's suitability for use in DMFC. The N-PVA/HPW20 membrane successfully recorded a peak power density of 2.7 mW cm^{-2}, which is 10.7% higher than the value of recast Nafion. Another highlight of these mixed-matrix membranes is their ability to recover up to 93% of their initial methanol barrier properties after being damaged. This fascinating self-healing property of the membrane is believed to have the potential to extend the service life of DMFC.

Keywords Proton exchange membrane (PEM) · Self-healing · Nafion · Phosphotungstic acid · Poly(vinyl alcohol) (PVA)

Introduction

Climate change and depletion of fossil fuel have forced the world to find mitigations to safeguard the environment while the world continues to strive for economic growth for its population [1]. Exploration into alternative energy sources such as fuel cells, which produce electricity from chemical energy without a combustion reaction, has caught a great deal of attention to address global energy and environmental issues. Fuel cells are a viable option for meeting the diversified energy demands of today in a variety of sectors. Several types of fuel cells have been developed based on the electrolytes used, for instance, solid oxide (SOFC), molten carbonate (MFC), and polymer electrolyte membrane fuel cell (PEMFC) [2]. Direct methanol fuel cell (DMFC), which is a subcategory of PEMFC, has gained considerable interest due to its relatively quick start-up, high power density, easy operation, and high energy conversion efficiency, all of which are generally applicable and advantageous in portable devices [3–6]. Additionally, substituting methanol for fossil fuel may favor decarbonization and satisfy energy needs.

One of the core components of DMFC, the proton exchange membrane (PEM), should significantly contribute to proton transport and prevent methanol fuel crossover through ionic channel. Nafion is the most commonly used PEM in DMFC because of its remarkable proton conductivity (0.01 S/cm) under hydrated conditions, as well as its excellent chemical and mechanical properties [7–10]. Nafion consists of a hydrophobic perfluorinated polyethylene backbone and hydrophilic sulfonic acid-terminated side chains. The sulfonic acid groups form a long-range

✉ Hui San Thiam
thiamhs@utar.edu.my

1 Lee Kong Chian Faculty of Engineering & Science, Universiti Tunku Abdul Rahman, Sungai Long Campus, Jalan Sungai Long, Bandar Sungai Long, Selangor 43000, Malaysia

2 Centre for Photonics and Advanced Materials Research, Universiti Tunku Abdul Rahman, Sungai Long Campus, Jalan Sungai Long, Bandar Sungai Long, Selangor 43000, Malaysia

proton-conducting channel for efficient proton transport, while the hydrophobic parts contribute to the outstanding mechanical integrity of the Nafion [11].

Despite the widespread acceptance of DMFC as a potential energy source, its viability must be enhanced due to the severe methanol permeability and long-term performance degradation of the Nafion membrane [12]. The ambiguity of the structural feature of Nafion impedes the scalability of DMFC application, as it favors protons for faster and more efficient transportation while promoting methanol permeation, which degrades cell performance. In hydrated state, the phase separation between hydrophobic and hydrophilic domains provides spaces for methanol diffusion. Therefore, methanol fuel can diffuse over the Nafion membrane along the concentration gradient. Moreover, electroosmosis drag, namely proton transportation along with solvent molecules like water and methanol, facilitates the penetration of methanol across PEM [13]. On the other hand, mechanical stress is also a factor that reduces the performance of Nafion membrane [14]. During fuel cell operation, Nafion membrane is subjected to fatigue stress as a result of variations in hydration level (wet and dry conditions), which cause the ionic cluster to expand and contract cyclically. Consequently, the continuous and repetitive swelling and shrinking trigger the formation of tears, microcracks, and pinhole in the Nafion membrane. These mechanical defects would cause devastating deterioration of the membranes and gradually reduce the lifetime of PEM.

In view of these circumstances, PEM is required to be assessed in terms of its methanol barrier properties and its capacity to repair mechanical damages in addition to proton conductivity. Extensive efforts have been carried out to improve the properties of PEM in DMFC, including the addition of inorganic material such as metal oxides and metal organic frameworks (MOFs) to create more winding and tortuous pathways [15–22], the introduction of other polymer with a methanol sieving effect [5, 23–26], and the modification of Nafion surface with a methanol barrier layer [27–29]. Recently, practices of incorporation of materials with low methanol compatibility have been reported in the literature. The low methanol compatible polymers include polyaniline, polypyrrole, poly(vinylidene fluoride) (PVDF), and poly(vinyl alcohol) (PVA). Particularly, PVA has been actively developed as a Nafion modifier [26, 30, 31], owing to its excellent film-forming characteristics, hydrophilicity, and higher selectivity of water towards alcohol [32–34]. In all the cases, lower methanol permeability was observed (up to 90% less than Nafion), although at the expense of conductivity loss (about half of Nafion). Another exciting discovery made in recent research demonstrated that Nafion-based membrane could acquire self-healing properties with the assistance of PVA [35]. PVA emerges as a self-healing polymeric material capable of executing self-repair in response to damages, hence extending membrane lifespan and restoring its original functionality. Even so, very limited papers reported on the self-healing mechanism of PEM during the DMFC operation.

Herein, we synthesized self-healable Nafion-PVA blend membranes through freezing–thawing approach and presented a method for tailoring the proton conductivity of Nafion-PVA membrane by incorporating heteropoly acids (HPAs) as proton carriers. Freezing–thawing can physically promote crosslinking in polymer without the need for chemical crosslinkers, whereas the HPAs, such as phosphotungstic acid (HPW), are Bronsted acids and well-known superionic proton conductors in the fully hydrated states and room temperature [36]. HPW has been shown to enhance water uptake and contribute to the construction of additional, interconnected channels for proton migration [4, 36]. According to a study by Pourzare et al. [37], the inclusion of HPW into Nafion increased the proton conductivity by 39% compared to pure Nafion. The advantages of HPA were also supported by the study proposed by Abouzari-Lotf et al. [38], whose membrane obtained a selectivity of 20 times higher than Nafion 115. Nevertheless, no research has been conducted on the PEM composed of Nafion, PVA, and HPW synthesized using the freeze–thaw method. Therefore, this work proposes Nafion-PVA blend membranes treated with HPW to impart self-healing property while simultaneously enhancing the selectivity of the membranes. The effects of various HPW loadings on membrane performance were also studied.

Experimental

Materials

Nafion dispersion (5% w/w in water and 1-propanol) and PVA (molecular weight of 146,000–184,000, > 99% hydrolyzed) were received from Thermo Fisher Scientific. Phosphotungstic acid hydrate ($H_3PW_{12}O_{40}.xH_2O$, HPW) and sulfuric acid (H_2SO_4, 95–98%) were purchased from Sigma-Aldrich, USA. Methanol (> 99.9%) was obtained from Merck, Germany. All chemical reagents were used without further purification.

Fabrication of membrane

Nafion-PVA blend membranes were prepared through a freezing–thawing process to induce physical crosslinking and self-healing properties without the use of chemical crosslinking agents. Firstly, a homogenous 5 wt% aqueous PVA solution was prepared by continuously heating and stirring 1 g of PVA in 20 mL of deionized water at 80 °C. Then, a mixture of Nafion and PVA solution at a weight ratio of 8:2 was prepared by heating Nafion dispersion to 70 °C and mixing it with an appropriate amount of PVA solution.

The mixture was then poured into a Teflon dish for casting, and a crosslinking network was established during freezing at − 20 °C for 24 h, followed by thawing at room temperature for 2 h, resulting in the formation of Nafion-PVA membranes (denoted as N-PVA). The membranes were subsequently dried at 65 °C for 15 h. Separately, an appropriate weight of HPW was dissolved in deionized water to obtain solutions with concentrations of 10 wt%, 20 wt%, and 30 wt%. The N-PVA membranes were then immersed for 24 h in the prepared HPW solutions to anchor the HPW into the polymer matrix. The resultant membranes were designated as N-PVA/HPWn, where *n* represents the weight percent of HPW solution. As a control, recast Nafion membrane was also prepared using the same procedure but without PVA and HPW. Prior to characterization testing, the synthesized membranes were activated by boiling in 1 M of sulfuric acid solution at 80 °C for 1 h, followed by multiple rinsing with deionized water [39].

Characterizations

Fourier transform infrared (FTIR)

The chemical structure of the membranes was determined using FTIR spectrometer (Nicolet iS10, Thermo Scientific) with ATR sampling technique. The FTIR spectra were obtained in the range of 400–4000 cm^{-1} at room temperature.

X-ray photoelectron spectroscopy (XPS)

X-ray photoelectron spectrometer (K-Alpha XPS, Thermo Scientic) was used to analyze the chemical composition of the membranes and confirm the incorporation of phosphotungstic acid. XPS spectra were collected at room temperature with X-ray source of Al Kα.

Thermal gravimetric analysis (TGA)

The thermal degradation behavior of the membranes was analyzed using a thermogravimetric analyzer (PerkinElmer, STA 8000) at temperatures ranging from 30 to 800 °C with a heating rate of 10 °C min^{-1} under nitrogen atmosphere.

Mechanical properties

The mechanical properties of the membranes were measured using a universal tensile machine (Shimadzu AGS-X) at room temperature. Before the measurement, the membrane was immersed in deionized water for 24 h at room temperature [40]. The membrane was then cut into 60 × 10 mm^2 rectangular strips with the gauge length set to 20 mm. After removing the surface water of the sample, the analysis was carried out at a crosshead speed of 2 mm min^{-1}.

Water uptake (WU) and methanol uptake (MU)

Water and methanol uptake of the membranes were determined by measuring their dry (W_{dry}) and wet weights (W_{wet}). The synthesized membrane was dried to a constant weight in an oven, and then, its weight was measured to obtain W_{dry}. The dried sample was then soaked in deionized water for 24 h at room temperature. After 24 h of immersion, the weight of the membrane was measured with the surface water removed using tissue papers to estimate W_{wet}. The water and methanol uptake were calculated using Eq. (1).

$$WU\ or\ MU\ (\%) = \frac{W_{wet} - W_{dry}}{W_{dry}} \times 100\% \quad (1)$$

Ion exchange capacity (IEC)

The membrane was dried to a constant weight prior to the test. To obtain the IEC, the membrane was immersed in a 2-M NaCl solution for 48 h to substitute all Na^+ ions with H^+ ions. Afterward, the obtained solutions were titrated and neutralized by a 0.01 M NaOH solution in the presence of a few drops of phenolphthalein indicator [41–43]. With the required volume of NaOH, the IEC was calculated using Eq. (2):

$$\mathrm{IEC}\,(mmol\ g^{-1}) = \frac{V_{NaOH} \times M_{NaOH}}{W_d} \quad (2)$$

where V_{NaOH} (mL) is the volume of consumed NaOH, M_{NaOH} (mol L^{-1}) is the molar concentration of NaOH, and W_d (g) is the dry weight of the membrane.

Proton conductivity

Before the test, the membrane was hydrated in deionized water for at least 24 h. Proton conductivity measurement was performed on the membrane in a four-probe cell using an electrochemical impedance technique based on the determination of the ohmic resistance of the membrane. By applying a current sweep from 0 to 15 mA with a scan rate of 0.25 mA/s, a graph of voltage against current was drawn. Equation (3) was used to determine proton conductivity:

$$\sigma\ (S\ cm^{-1}) = \frac{L}{R \times w \times t} \quad (3)$$

where σ is the proton conductivity, L (cm) is the distance between two inner electrodes, R (Ω) is the membrane resistance (or the gradient of the graph), w (cm) is the width of the membrane, and t (cm) is the thickness of the membrane.

Methanol permeability

A two-compartment diffusion cell was used to measure the permeation of methanol through the synthesized membranes.

Before the experiment, the membrane was equilibrated in deionized water for 24 h. One compartment (A) of the cell was filled with a 2-M methanol solution, while the other compartment (B) contained deionized water. Both compartments held the same volume of liquids. Throughout the experiment, the liquids in both compartments were continuously stirred to maintain concentration uniformity. Multiple samples of solution from compartment B were extracted at different times, and their methanol concentrations were determined using a gas chromatography. The methanol permeability, P_M, of the membrane was calculated using Eq. (4):

$$P_M\left(cm^2\,s^{-1}\right) = \frac{SVt}{C_{MO}A} \tag{4}$$

where S (M s^{-1}) is the rate of change of methanol concentration in compartment B, V (cm^3) is the volume of solution in each compartment, t (cm) is the membrane thickness, C_{MO} (M) is the initial concentration of methanol solution, and A (cm^2) is the membrane effective area.

Selectivity

Selectivity is a crucial factor in characterizing and comparing the overall performance of PEM in DMFC by calculating the ratio between proton conductivity and methanol permeability, as shown in Eq. (5). A high selectivity ratio is desirable as it implies better electrochemical performance.

$$\varnothing\left(S\,s\,cm^3\right) = \frac{\sigma}{P_M} \tag{5}$$

where $\varnothing$ is the selectivity, σ is the proton conductivity, and P_M is the methanol permeability.

Self-healing

Self-healing ability of the membrane was determined by first making a few holes in the membrane and then immersing it in a 2-M methanol solution for 4 h for healing purpose. After the healing process, the conditions of the membrane were examined using scanning electron microscopy (SEM). To measure the self-healing ability quantitatively, the methanol permeability test was performed on the damaged and healed membranes.

Passive DMFC performance

The fuel cell performance test was carried out using an air-breathing single cell. The membrane was sandwiched between anode and cathode catalyst layers by hot press at 135 °C under 20 kg cm^{-2} for 2 min. The anode and cathode contain 4 mg cm^{-2} of PtRu and Pt, respectively. Effective membrane electrode assembly (MEA) surface area was 2×2 cm^2. The performance of the membrane in DMFC was evaluated at room temperature with a 2-M and 4-M methanol feed solution at the anode and air at the cathode.

Results and discussion

FTIR

The chemical structures of pristine Nafion, HPW, N-PVA, and N-PVA/HPW membranes were compared based on FTIR spectroscopy (Fig. 1). For the recast Nafion membrane and N-PVA/HPW mixed-matrix membranes, the bands at 460 cm^{-1} and 1056 cm^{-1} corresponded to the symmetric stretching vibration of O–S–O and S–O, respectively. Meanwhile, the peaks identified at 1200 cm^{-1} and 1144 cm^{-1} represented, respectively, the asymmetric and symmetric stretching of S–O of the sulfonic groups in Nafion [44]. Moreover, the characteristic peak at 969 cm^{-1} was assigned to the stretching vibrations of C–O–C groups, and the band observed at 632 cm^{-1} was attributed to the C–S stretching. On the other hand, N-PVA blend membrane and N-PVA/HPW mixed-matrix membranes possessed broad transmission peaks between 3300 and 3600 cm^{-1} and 2923 and 2942 cm^{-1} which were ascribed to O–H stretching of hydroxyl groups and asymmetric C–H stretching, respectively, both indicating successful incorporation of PVA into the Nafion polymer matrix [45]. HPW is made of central PO_4 tetrahedron units surrounded by tungsten (W_3O_{13}) units and connected by oxygen atoms [46, 47]. Hence, there were four W–O characteristic stretching peaks displayed by the FTIR spectrum of pure HPW, which appeared at 1072 cm^{-1} (P–O_a), 972 cm^{-1} (W–O_d terminal oxygen), 899 cm^{-1} (W–O_b–W corner oxygen) and 746 cm^{-1} (W–O_c–W edge oxygen) [33, 48–51]. It could be observed that the FTIR spectrum of N-PVA/HPW in the region between 500 and 1250 cm^{-1} was quite similar to the pristine HPW, with the bands at 823 cm^{-1} and 1093 cm^{-1} standing out due to the stretching mode of HPW. Compared with pure HPW, N-PVA/HPW revealed shifting in peak positions and a decrease in peak intensity, signifying the possibility of hydrogen bonding and ionic interactions between HPW and functional groups in Nafion and PVA [36, 48]. N-PVA/HPW also demonstrated a shallower O–H band, indicating that the mixed-matrix membrane was more hydrophilic due to the presence of water crystals inside the crystal structure of HPW [51, 52].

XPS

XPS was used to determine the electronic states and chemical composition of N-PVA/HPW20 membrane. The characteristic peaks in XPS analysis (Fig. 2a) showed the presence of five relative elements within the energy range from 30 to 700 eV, including carbon (C1s), oxygen (O1s),

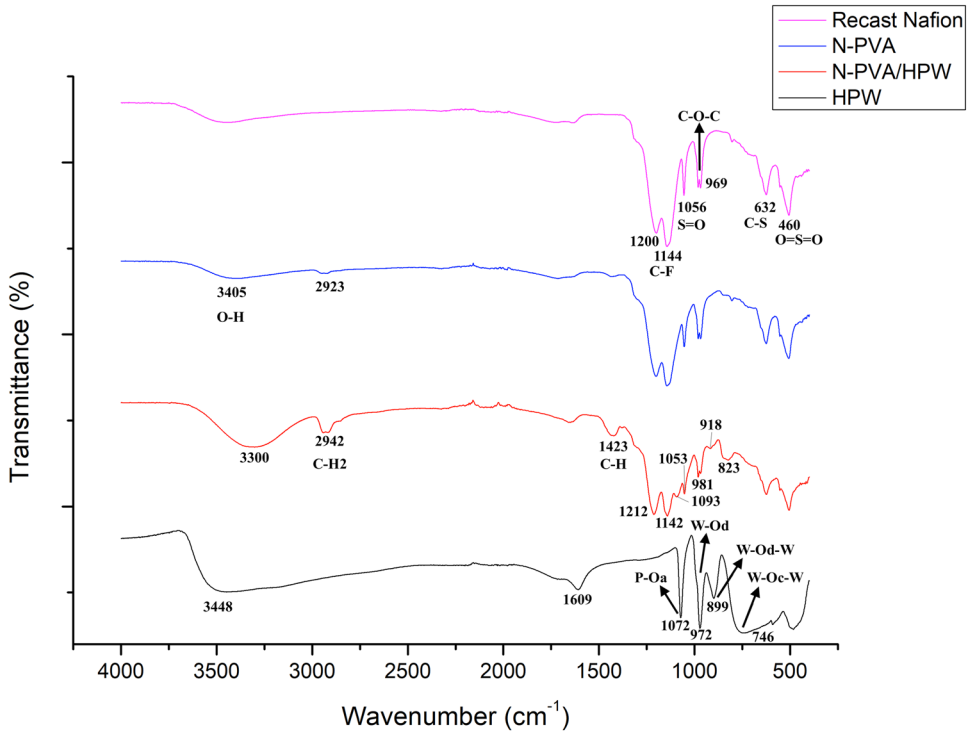

Fig. 1 FTIR spectra of recast Nafion, N-PVA, N-PVA/HPW membranes, and pure HPW

fluoride (F1s), sulfur (S2p), and tungsten (W4f). The C1s (Fig. 2b) was attributed to the alkyl carbon peak (C–C) and the ether carbon peak (C–O), which were observed at 290.1 eV and 291.6 eV, respectively [53, 54]. Also, the peak around 293.9 eV and 296.5 eV was ascribed to C–F groups in Nafion [55]. The O1s spectra (Fig. 2c) could be used to infer several contributions from different chemical functional groups. The peaks detected at 542.3 eV, 539.8 eV, and 537.1 eV corresponded to the oxygen series present in the ether functional group (C–O–C and C–O) and sulfonate group (SO_3^-) [56, 57]. Meanwhile, the sulfur in the sulfonate group of Nafion was shown by the peak at 173.7 eV in the S2p [50, 58] (Fig. 2d). The peak of F1s spectra (Fig. 2e) at 693.1 eV is assigned to CF_2 or CF_3 groups in Nafion [54]. Lastly, the binding energy peak of W4f centered at 37.8 eV, which are attributed to the $PW_{12}O_{40}^{3-}$ in the Keggin structure of HPW [59], can be seen in W4f spectra (Fig. 2f), confirming the existence of W element in the sample.

TGA

Thermal stabilities of recast Nafion, N-PVA, and N-PVA/HPW membranes were analyzed, and the results are shown in Fig. 3. Nafion membrane exhibited three main degradation stages whereas the N-PVA blend membrane and N-PVA/HPW mixed-matrix membranes share similar degradation trend which consists of four steps of weight loss. The first weight loss for all samples at around 100 °C was attributed to the evaporation of water and solvents. The second degradation of the N-PVA and N-PVA/HPW membranes starting from around 110 to 350 °C was correlated to the dehydration of hydroxyl groups from PVA [60]. The third weight loss region of mixed-matrix membranes between 350 and 450 °C indicated the degradation of sulfonic acid groups, while in recast Nafion, this was found between 300 and 400 °C. Compared to recast Nafion, the desulfonation temperature of mixed-matrix membranes was delayed, demonstrating greater thermal stability. Moreover, as the filler percentage of HPW increased, the weight loss decreased, showing that the thermal stability of the N-PVA/HPW membranes increased with HPW loading. The last stage of weight loss, the decomposition of the polymer main chains, occurred after 420 °C for recast Nafion and 450 °C for N-PVA/HPW membranes resulted in the most significant weight loss [61]. The greater thermal stability of the N-PVA/HPW membranes, as seen in Fig. 3, can be explained by the presence of the inorganic filler, which may interact with the sulfonic acid groups and therefore restrict the mobility of the polymer chains. Based on the TGA findings, the mixed-matrix membranes are thermally stable at temperatures below 250 °C, making them suitable for use in high-temperature DMFC.

Water and methanol uptake

Water and methanol uptake of recast Nafion, N-PVA, and N-PVA/HPW membranes with varying concentrations of HPW are expressed in Fig. 4. Adequate water uptake is

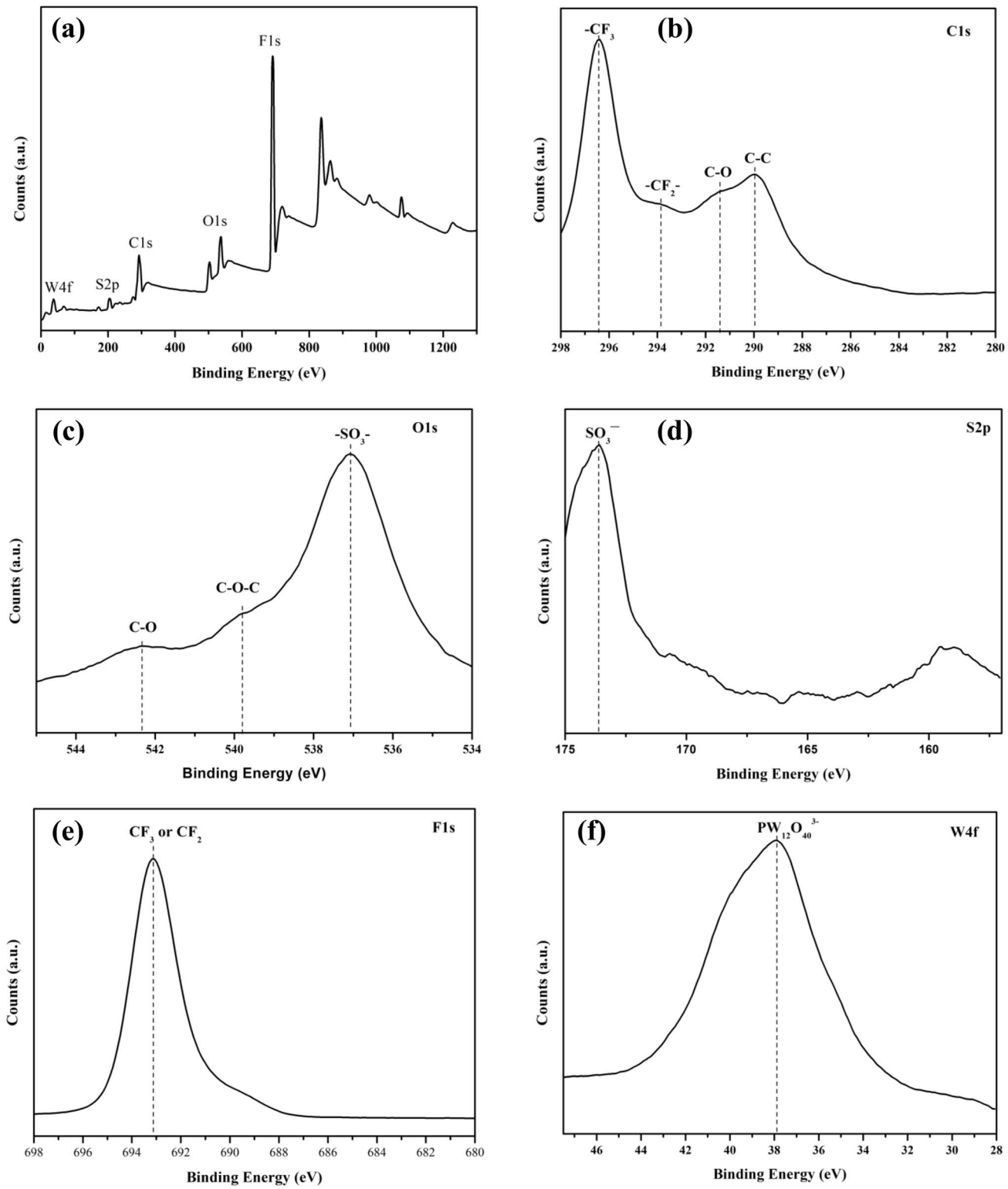

Fig. 2 XPS analysis of **a** survey spectra, **b** C1s, **c** O1s, **d** S2p, **e** F1s, and **f** W4f spectra of N-PVA/HPW20 membrane

crucial for proton transport because water molecules act as proton carriers; protons combine with water molecules to form hydrated protons (H_3O^+), which are then transported across the PEM [45]. Higher water uptake aids proton transport through diffusion; however, excessive water uptake can negatively affect the methanol barrier properties and mechanical strength of the membrane. From the results of water uptake by mixed-matrix membranes, an increasing

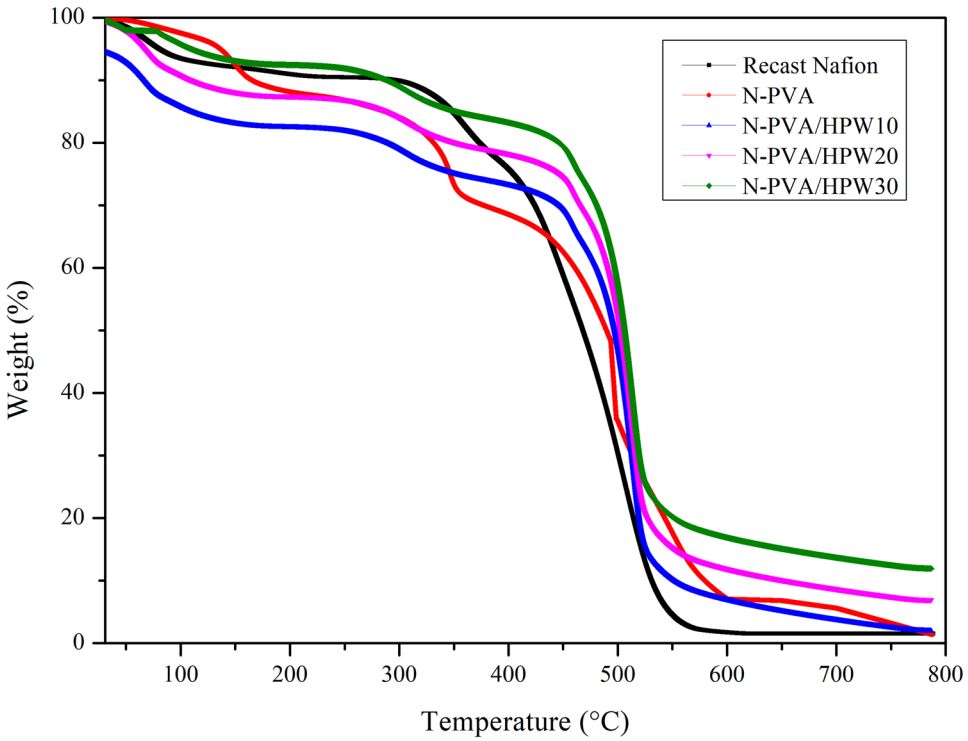

Fig. 3 TGA analysis of Nafion 117, N-PVA, and N-PVA/HPW membranes

trend was noticed as the membranes were treated with a higher concentration of HPW. Of the prepared N-PVA/HPW membranes, N-PVA/HPW30 demonstrated the highest water uptake at 132.3%, which was around 6.4 times higher than recast Nafion (20.8%). The increment could be deduced from the hydrophilicity nature of HPW, and when the concentration of HPW in the treatment solution increased, more HPW was incorporated into the membrane. Having an abundance of O atoms, HPW interacts with water molecules through weak hydrogen bonding, which facilitates water adsorption of the mixed-matrix membranes [62]. Besides, the heteropolyanion groups $[PW_{12}O_{40}]^{3-}$ (also

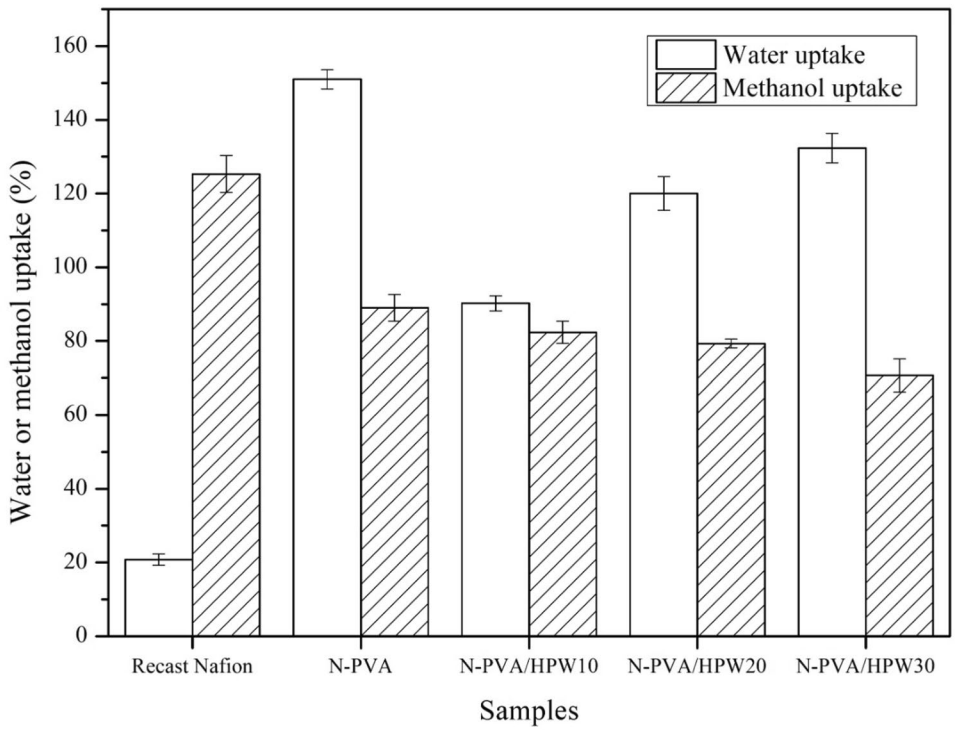

Fig. 4 Water and methanol uptake of recast Nafion, N-PVA, and N-PVA/HPW membranes

known as Keggin anion) in HPW are capable of attracting a large amount of water molecules into the membrane [36, 46]. However, the water absorption site in the mixed-matrix membrane might be reduced due to the interactions between the hydroxyl groups in PVA blend and the terminal oxygen and the bridging oxygen in HPW [60]. This explains why the water sorption of mixed-matrix membranes was lower than that of N-PVA membrane (lowered by 1.14 to 1.67 times).

Methanol uptake is one of the key properties for PEM performance in DMFC, as it may reflect the methanol permeability of PEM. Low methanol uptake is favorable for reducing methanol loss across the membrane. Notably, the sorption ability of N-PVA/HPW membranes in methanol decreased from 82.4 to 70.7% as the HPW concentration increased. In addition, the methanol uptake of the three N-PVA/HPW membranes was lower than that of the N-PVA and the recast Nafion membranes. This behavior inferred that the addition of HPW promoted the electrostatic interaction and hydrogen bonding (between sulfonic groups and HPW, as well as between PVA and HPW), which led to a denser, more compact structure and the formation of a channel barrier. Additionally, the HPW disrupted the methanol transport pathway by blocking the voids of N-PVA/HPW matrix as a result of the larger Keggin anion in HPW [63].

Mechanical properties

Mechanical properties of membrane are related to both temperature and water content. Membrane must have strong mechanical properties to withstand high compression for MEA fabrication [43]. Table 1 shows the tensile strength of pure Nafion, N-PVA, and N-PVA/HPW membranes in wet condition. The tensile strength of N-PVA reduced by about 43.4% after the addition of PVA into recast Nafion. However, by treating the membrane with HPW solutions, the tensile strength was enhanced by 15.5 to 78.6%, with the largest improvement occurring in the N-PVA membrane treated with a 10 wt% HPW solution. The improvement was due to the formation of dynamic hydrogen bonds between the sulfonic acid groups in Nafion, the hydroxyl groups in PVA, and the oxygen-containing groups in HPW, which increased the crosslinking degree and created a compact structure [64]. However, the mechanical properties deteriorated with increasing HPW content. This was likely because the hydrophilic PVA and HPW absorbed more water within the membranes. In comparison to N-PVA, the elongation of N-PVA/HPW decreased by at least 26.2% with increasing tensile strength, as the addition of HPW increased the stiffness of the membrane by increasing crosslinking and subsequently decreasing the mobility of the polymer chain, which could be proven by the increment in the value of Young's modulus. In short, the mixed-matrix membranes are ductile and meet the mechanical requirements for MEA fabrication [43, 65].

IEC

IEC evaluates the surface charge of the membrane, which reveals its proton exchangeable capacities and, hence, its ability to conduct protons [33, 66]. The higher IEC value indicates the dominance of the Grotthuss mechanism, which favors the transfer of proton via proton hopping. However, excessive hydrophilic ion-conducting groups will inevitably increase water uptake and lead to mechanical degradation of the membrane. As expected, the IEC of the mixed-matrix membranes increased gradually with increasing HPW content. According to Table 2, among the modified membranes, N-PVA/HPW30 showed the highest IEC value of 1.12 mmol g^{-1}, which is comparable to the value of recast Nafion (1.04 mmol g^{-1}). Although the IEC of the N-PVA/HPW10 (0.78 mmol g^{-1}) and N-PVA/HPW20 (0.95 mmol g^{-1}) membranes was lower than recast Nafion membrane, their IEC values were superior to those of the N-PVA (0.73 mmol g^{-1}) membrane. This phenomenon is related to the enrichment of hydrophilic functional groups found in HPW. The strong acidity of HPW arises from the presence of polyanion $[PW_{12}O_{40}]^{3-}$, which significantly increases the positive charge accumulated on its surface [47]. As a result of the increasing charge, the IEC rises, which is favorable for the functioning of the fuel cell.

Proton conductivity

Proton conductivity correlates to the availability of ion exchange sites and water content of a membrane. This is because proton transport occurs through the Grotthuss mechanism, in which protons jump from one anionic group to the other via the formation and cleavage of hydrogen bonds; meanwhile, the vehicular mechanism involves the diffusion

Table 1 Mechanical properties of recast Nafion, pristine N-PVA, and N-PVA/HPW membranes

Sample	Thickness (mm)	Tensile strength (MPa)	Elongation (%)	Young's modulus (MPa)
Recast Nafion	0.20	6.36 ± 0.38	45.62 ± 4.70	14.27 ± 2.28
N-PVA	0.20	2.76 ± 0.23	88.43 ± 2.60	6.07 ± 0.51
N-PVA/HPW10	0.18	4.93 ± 0.96	61.43 ± 7.19	8.09 ± 1.78
N-PVA/HPW20	0.18	3.97 ± 0.01	63.90 ± 6.22	6.25 ± 0.60
N-PVA/HPW30	0.18	3.19 ± 0.69	65.25 ± 1.72	6.12 ± 0.13

Table 2 IEC of recast Nafion, pristine N-PVA membranes, and N-PVA treated with different weight percent of HPW solutions

Sample	Recast Nafion	N-PVA	N-PVA/HPW10	N-PVA/HPW20	N-PVA/HPW30
IEC (mmol g^{-1})	1.04	0.73	0.78	0.95	1.12

of protons together with water molecules [67]. As depicted in Fig. 5, the addition of PVA reduced the concentration of the sulfonic acid moiety required for proton transport, resulting in a considerable decrease in proton conductivity for N-PVA membrane. However, after treating with HPW, proton conductivity was shown to be higher in all modified samples compared to the N-PVA membrane. This trend was more pronounced as the HPW content was higher, in agreement with the literature documented by Mohanapriya et al. [63]. The N-PVA/HPW30 membrane achieved the highest proton conductivity of 0.073 S cm^{-1}, which was mainly attributed to two possible reasons: (1) hydrophilic HPW exhibited high water uptake and (2) additional proton exchange sites provided by HPW. With increased water molecule absorption, protons might migrate more easily via vehicular mechanism [66]. Besides, the unique structure of HPW, which consists of anion groups, can contribute to the preferential proton transport, as protons can be coordinated to the oxygen atoms in HPW. The anion groups of HPW can also combine with hydrated protons (H_3O^+), allowing hydronium ions to jump from one HPW to the neighboring HPW along the water-associated hydrogen bond [47]. Thus, the proton transmission is accomplished not only by the sulfonic acid groups but also the anion groups in HPW [51, 68, 69]. In a word, the strong intrinsic water absorption capacity and additional O sites of HPW promote the movement of proton along the PEM.

Methanol permeability

Another factor that might affect the performance of a PEM is the methanol crossover. The structural motifs of Nafion lead to a high methanol permeability [9], which can result in several adverse effects, for instance, a decrease in fuel efficiency, overpotential, cathode catalyst poisoning, and eventually depress the performance of DMFC. Figure 6 demonstrates that methanol permeability increased with increasing HPW content because the membrane became more hydrophilic, as evidenced by the water uptake test results. The highest methanol permeability was observed for the N-PVA/HPW30 membrane at 3.2×10^{-6} cm^2 s^{-1}, compared to the N-PVA (2.15×10^{-6} cm^2 s^{-1}), N-PVA/HPW10 (2.38×10^{-6} cm^2 s^{-1}), and N-PVA/HPW20 (2.74×10^{-6} cm^2 s^{-1}). HPW is well-known for its high water uptake capacity, which facilitated methanol diffusion and caused the undesired methanol permeability. Despite the minor drop in the methanol uptake upon treatment with a higher concentration of HPW, the drastic increase in water absorption might widen the free volume of the polymer matrix, reduce the dimensional stability, and contribute to a loose structure, thereby reducing the methanol hindering effect [51, 69]. Nevertheless, the methanol

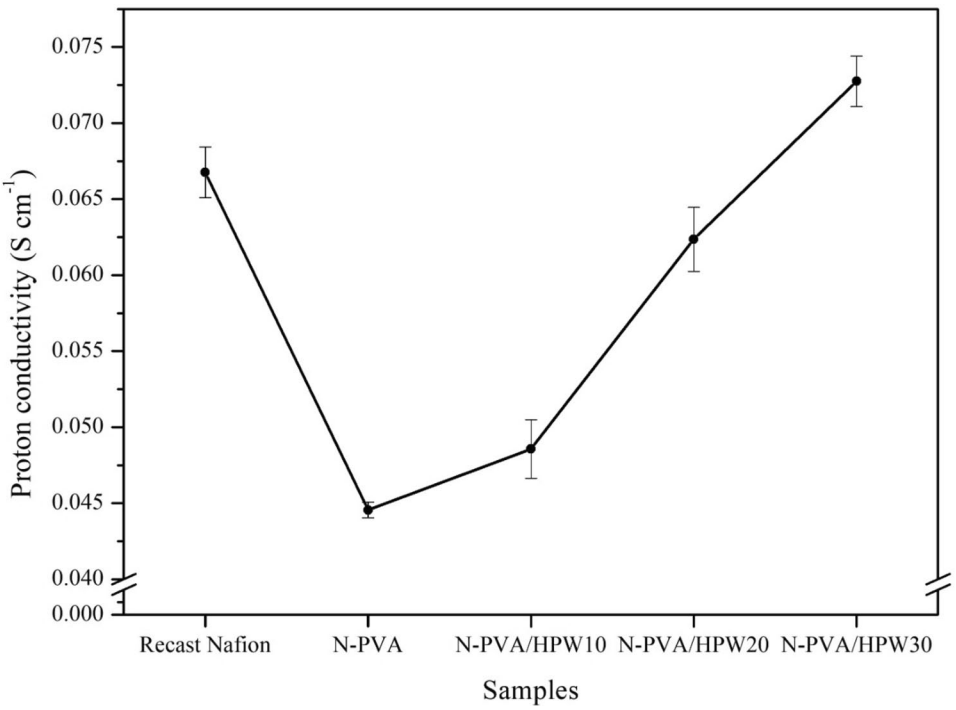

Fig. 5 Proton conductivity of recast Nafion, N-PVA, and N-PVA/HPW membranes

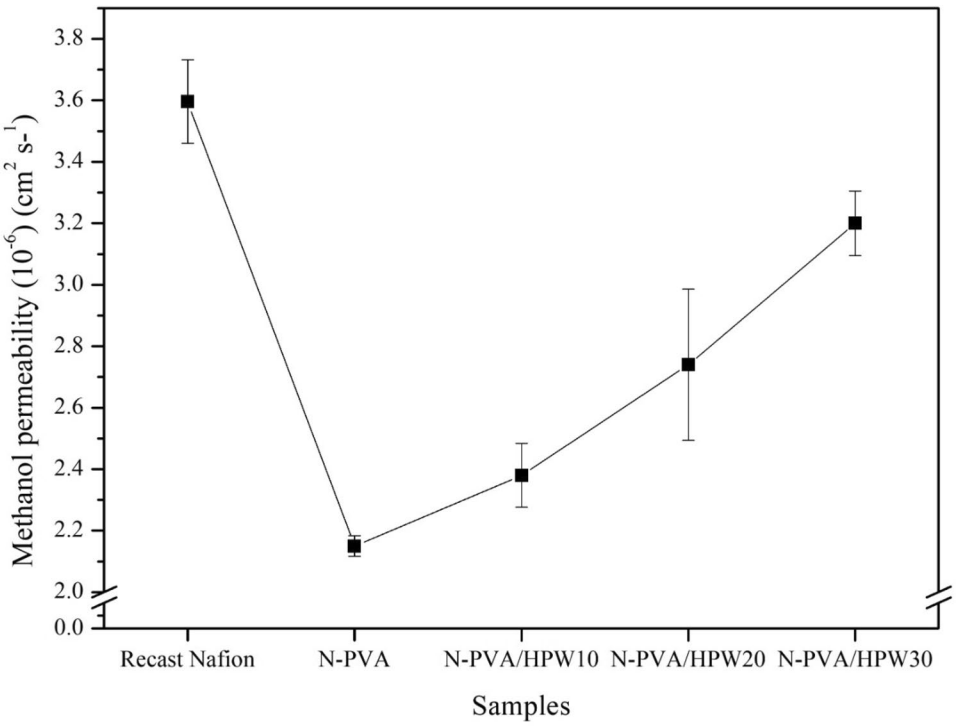

Fig. 6 Methanol permeability of recast Nafion, N-PVA, and N-PVA/HPW membranes

permeability of the HPW-modified membranes was lower than that of recast Nafion (3.6×10^{-6} cm^2 s^{-1}). This could be explained by the unique phase-separated nanostructure of Nafion, which is formed by the hydrophobic perfluorinated backbone and hydrophilic sulfonic acid groups [70]. The separation of the domains allowed the movement of methanol molecules, yielding a higher methanol permeability in Nafion. On the other hand, the interaction of HPW with the blend membrane suppressed the phase separation of N-PVA/HPW, forming a relatively packed structure; therefore, methanol diffusion would be limited [71].

Self-healing

Formation of mechanical damage is another major concern when developing PEM. This is a key factor to consider when operating PEM under cyclical swelling and shrinking conditions. Thanks to the presence of PVA and its high degree of hydrophilicity, PEM could be endowed with self-healing properties. Figure 7 shows that all the PVA-loaded membranes could repair the damages on the membranes after 4 h of self-healing process in a methanol solution. The membranes were also subjected to a methanol permeability test to determine whether their original methanol-blocking properties could be restored. As illustrated in Fig. 8, the healed PVA-modified membranes demonstrated a methanol permeability value comparable to that of the respective original, undamaged membranes. N-PVA, N-PVA/HPW10, N-PVA/HPW20, and N-PVA/HPW30 recovered 86%, 83%, 85%, and 93% of the methanol barrier function of intact membranes, respectively. This implied that PVA possessed a great potential to serve as a self-healing material. During the process, the fracture surface was brought into contact by the methanol solution, and the broken chain migrated from one side to the other to promote the reformation of hydrogen bonds [72]. This interaction ended up joining the broken parts and allowed the restoration of the hydrogen bonds between PVA chains, Nafion, and HPW. Specifically, the recoverability of the N-PVA/HPW30 membrane increased drastically to 93%, which could be attributed to the higher water holding capacity that rendered the higher polymer chain mobility. This promoted chain diffusion across the cut interface and increased the efficiency of self-healing. However, the high water uptake caused by the HPW's superior acidity and unique structure (protonic Keggin-type polyoxometalates) would result in severe methanol crossover [68]. Since HPW has an antagonistic effect on self-healing ability and methanol permeability, it is important to strike a balance between these two characteristics by controlling the HPW loading in a membrane to avoid negatively impacting PEM performance.

Selectivity

PEMs are always confronted with a trade-off between membrane proton conductivity and methanol permeability as they are two inter-related phenomena. The factors which hinder the flow of methanol molecules through a PEM also impede the transport of water molecules and associated protons. Thus,

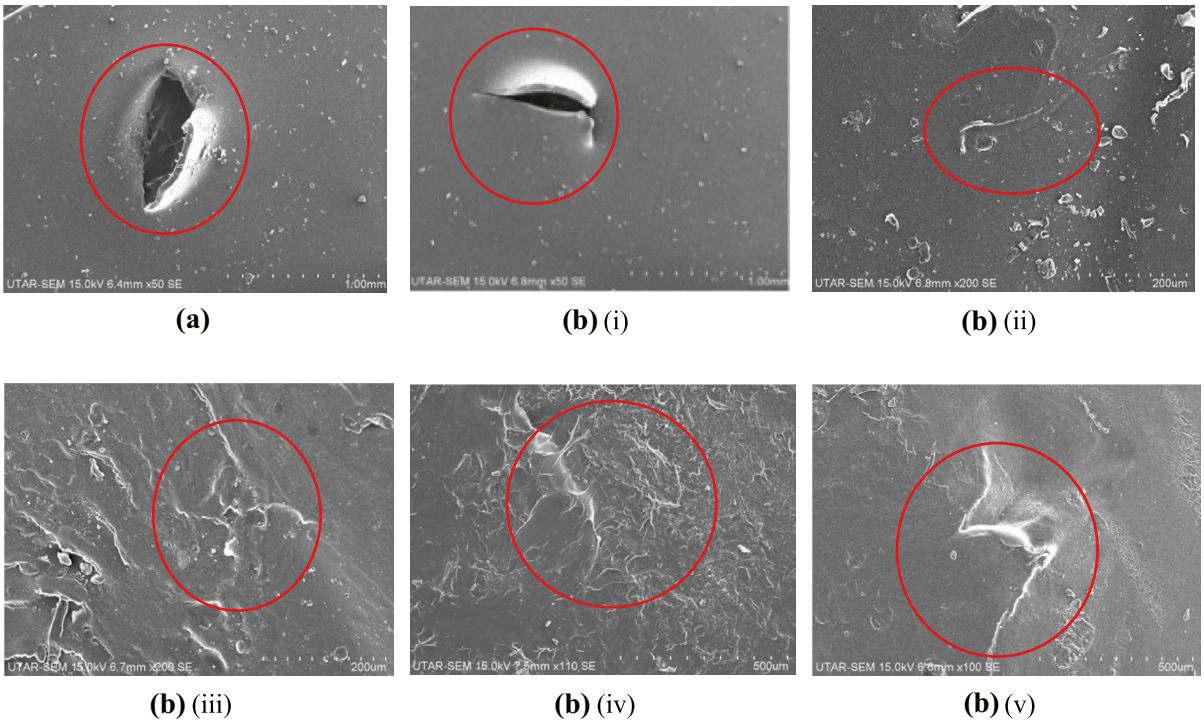

Fig. 7 SEM image of **a** damaged membrane, as well as **b** (**i**) recast Nafion, (**ii**) pristine N-PVA, (**iii**) N-PVA/HPW10, (**iv**) N-PVA/HPW10, and (**v**) N-PVA/HPW30 after healing process

effort has been devoted in PEM with augmented ionic conductivity without compromising the desirable methanol barrier properties. Typically, selectivity, defined as the ratio of proton conductivity to methanol permeability, is used as the performance metric for PEM in DMFC. In general, a higher selectivity suggests that it would be an excellent PEM candidate. As shown in Fig. 9, the selectivity of HPW-modified membranes exceeded that of unmodified Nafion and N-PVA membranes. The N-PVA/HPW20 membrane demonstrated the highest selectivity with 2.2759×10^4 S s cm^3 because of its

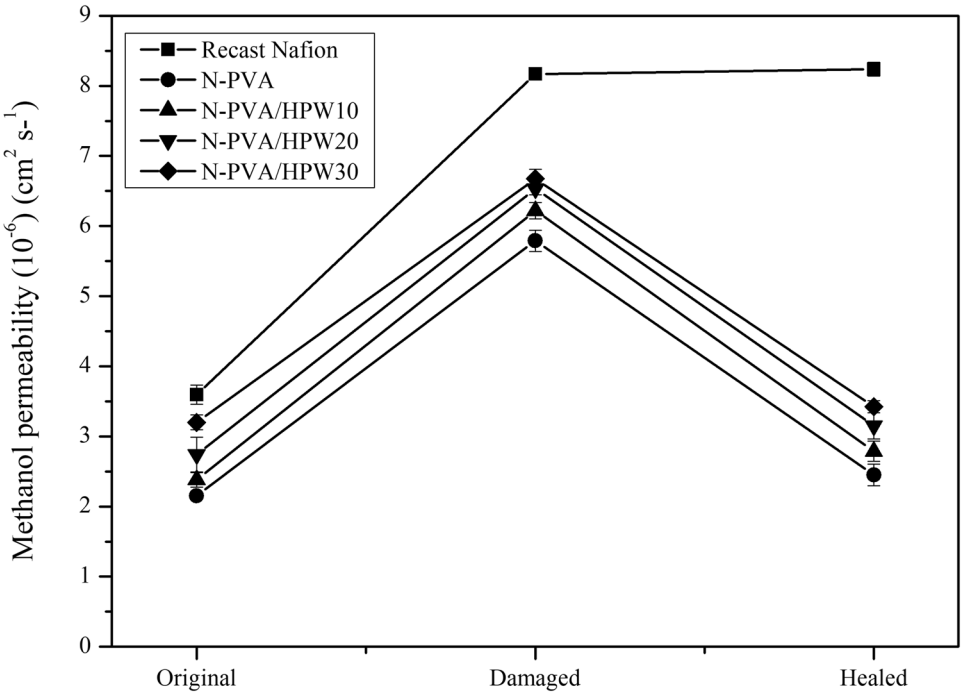

Fig. 8 Methanol permeability of original, damaged, and healed recast Nafion, N-PVA, and N-PVA/HPW membranes

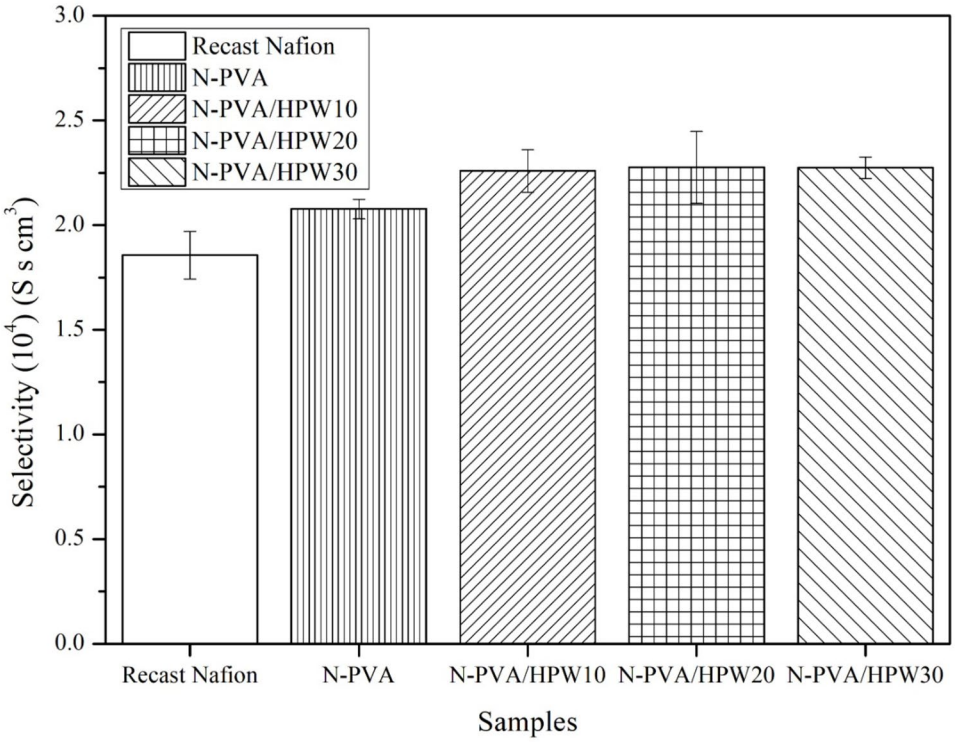

Fig. 9 Selectivity of recast Nafion, N-PVA, and N-PVA/HPW membranes

acceptable proton conductivity and tolerable methanol permeability. The synergy effect of heteropoly acid and PVA for proton conductivity improvement and methanol barrier properties was evidenced by the fact that N-PVA/HPW20 provided new sites for proton transfer and reduced opportunity for the methanol permeation. HPW also contributed to the enhancement in water holding capacity that assisted in proton diffusion. In contrast, the selectivity of pristine Nafion membrane under the same conditions was 1.8568×10^4 S s cm^3, which was 18.4% lower than N-PVA/HPW20, as the result of the high methanol permeability issue. Thus, N-PVA/HPW20 is seen as a promising alternative for use in DMFC applications due to the superior

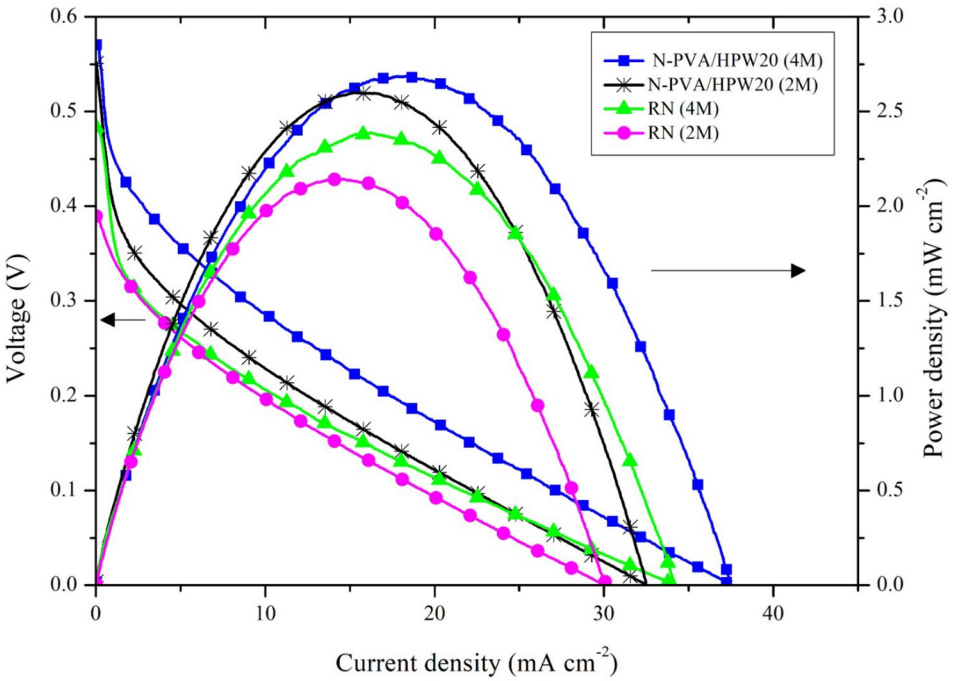

Fig. 10 Polarization curves of recast Nafion and N-PVA/HPW20 membranes

Table 3 Comparison of the passive DMFC performance of various Nafion-based membranes

Sample	Catalyst loadings (mg cm^{-1})		Methanol concentration (M)	Current density (mA cm^{-2})	Power density (mW cm^{-2})	Reference
	Anode	Cathode				
Nafion/silica/polyaniline	4 – 80wt% PtRu/C	4 – Pt/C	2	~17	5	[73]
Nafion 115	4 – 1:1At% PtRu/C	2 – Pt/C	2	-	3.3	[74]
Analcime/Nafion	2 – PtRu/C	0.5 – 60% Pt/C	4	~20	2.86	[75]
N-PVA/HPW20	4 – PtRu/C	4 – Pt/C	4	17.92	2.70	This work
Nafion 117	2 – PtRu/C	0.5 – 60% Pt/C	4	~20	2.68	[75]
Nafion 117	2 – PtRu/C	0.5 – 60% Pt/C	2	~16	2.56	[75]
Recast Nafion	4 – PtRu/C	4 – Pt/C	4	16.26	2.41	This work
Nafion 117	4 – 50% PtRu/C	2 – 50% Pt/C	4	~15	2.2	[76]
Nafion 117	2 – 20wt% 1:1At% PtRu/C	2 – Pt/C	3	0.112	2.2	[77]
Nafion 117	-	-	3	-	2	[78]

selectivity of the mixed-matrix membrane and its unique self-healing feature, which should increase the lifetime of DMFC.

Passive DMFC performance

It is well understood that a higher selectivity value results in a better membrane performance in DMFC. Hence, to elucidate the improvement in selectivity in this work, N-PVA/HPW20 was compared to the pristine Nafion membrane in a single-cell DMFC operating at room temperature and ambient pressure. Since the methanol concentration has a significant effect on electrical performance, two different methanol feed solutions were tested, with a concentration of 2 M and 4 M. The corresponding polarization and power density curves are displayed in Fig. 10. The output trend was the same for both membranes, with an increase in OCV and power density as methanol concentration was increased from 2 to 4 M. Using a 4-M methanol solution, N-PVA/HPW20 delivered a peak power density of 2.70 mW cm^{-2} at a load current density of 17.92 mA cm^{-2}, while DMFC assembled with recast Nafion membrane produced a maximum power density of 2.41 mW cm^{-2} at a limiting current of 16.26 mA cm^{-2}. The lower performance observed with recast Nafion was probably due to the high rate of fuel crossover from anode to cathode. This again confirms that the reduced methanol permeability of the mixed-matrix membrane improved DMFC performance. With its decreased permeability to methanol, the mixed-matrix membrane can be used in DMFCs with a high methanol concentration, hence increasing the power output. Table 3 compares the performance of passive DMFC of several Nafion-based membranes. The findings of this study are generally in agreement with the existing literature. Nonetheless, due to the variation in process parameters across research, it is difficult to draw any solid comparisons or conclusions.

Conclusion

For the purpose of creating a new self-healable mixed-matrix membrane, this study describes the synthesis of N-PVA membrane and its subsequent treatment with varying concentrations of HPW, as well as the resulting PEM properties. The results showed that the membrane properties such as water uptake, IEC, and proton conductivity were improved. The highest selectivity was achieved by N-PVA/HPW20 at 2.2759×10^4 S s cm^3 because of the interactions between the N-PVA blend and the $[PW_{12}O_{40}]^{3-}$ anion through hydrogen bonds, which compact the structure and diminish the effect of the methanol crossover. In addition, the proton conductivity (0.062 S cm^{-1}) was moderately increased due to the hydrophilicity of HPW, which enhanced the water uptake of the membrane, while the polyanions of HPW provided more ionic exchangeable sites for proton transfer. In addition to its superior selectivity, the N-PVA/HPW20 membrane also demonstrated remarkable self-healing properties by recovering 85% of its original methanol blocking function thanks to the reversible hydrogen bonds provided by PVA. Furthermore, HPW strengthened the mixed-matrix membrane thermally and mechanically. By the combined efforts of lower methanol permeability and comparable proton conductivity, the passive single cell based on N-PVA/HPW20 exhibited maximum power density of 2.7 mW cm^{-2}. In summary, the promising characterization results of N-PVA/HPW20 validated its prospective applicability as a PEM candidate in DMFC.

Author contribution Wei Wuen Ng: methodology, investigation, writing-original draft. Hui San Thiam: conceptualization, writing-review and editing, funding acquisition. Yean Ling Pang: writing-review and editing, supervision. Yun Seng Lim: resources, supervision. Jianhui Wong: conceptualization, funding acquisition.

Funding This research was supported by the Ministry of Higher Education (MoHE), Malaysia, through the Fundamental Research Grant Scheme (FRGS/1/2021/TK0/UTAR/02/20), and the Universiti Tunku Abdul Rahman (UTAR) Research Grant (IPSR/RMC/UTARRF/2021-C1/T06).

References

1. Liu Y-R, Chen Y-Y, Zhuang Q, Li G (2022) Recent advances in MOFs-based proton exchange membranes. Coord Chem Rev 471:214740. https://doi.org/10.1016/j.ccr.2022.214740
2. Ng WW, Thiam HS, Pang YL, Chong KC, Lai SO (2022) A state-of-art on the development of Nafion-based membrane for performance improvement in direct methanol fuel cells. Membranes 12(5):506. https://doi.org/10.3390/membranes12050506
3. Muhmed SA, Jaafar J, Daud SS, Hanifah MFR, Purwanto M, Othman MHD, Rahman MA, Ismail AF (2021) Improvement in properties of nanocrystalline cellulose/poly (vinylidene fluoride) nanocomposite membrane for direct methanol fuel cell application. J Environ Chem Eng 9(4):105577. https://doi.org/10.1016/j.jece.2021.105577
4. Zaffora A, Di Franco F, Gradino E, Santamaria M (2020) Methanol and proton transport through chitosan-phosphotungstic acid membranes for direct methanol fuel cell. Int J Energy Res 44(14):11550–11563. https://doi.org/10.1002/er.5777
5. Wang H, Li X, Feng X, Liu Y, Kang W, Xu X, Zhuang X, Cheng B (2018) Novel proton-conductive nanochannel membranes with modified SiO_2 nanospheres for direct methanol fuel cells. J Solid State Electrochem 22(11):3475–3484. https://doi.org/10.1007/s10008-018-4057-1
6. Chia MY, Thiam HS, Leong LK, Koo CH, Saw LH (2020) Study on improvement of the selectivity of proton exchange membrane via incorporation of silicotungstic acid-doped silica into SPEEK. Int J Hydrogen Energy 45(42):22315–22323. https://doi.org/10.1016/j.ijhydene.2019.11.010
7. Shi G-Q, Tao Z-X, Wang Q-X, Li G (2022) Proton conduction in two highly stable cadmium(II) metal-organic frameworks built by substituted imidazole dicarboxylates. J Solid State Chem 309:122948. https://doi.org/10.1016/j.jssc.2022.122948
8. Liu S-S, Liu Q-Q, Huang S-Z, Zhang C, Dong X-Y, Zang S-Q (2022) Sulfonic and phosphonic porous solids as proton conductors. Coord Chem Rev 451:214241. https://doi.org/10.1016/j.ccr.2021.214241
9. Al Munsur AZ, Goo BH, Kim Y, Kwon OJ, Paek SY, Lee SY, Kim HJ, Kim TH (2021) Nafion-based proton-exchange membranes built on cross-linked semi-interpenetrating polymer networks between poly(acrylic acid) and poly(vinyl alcohol). ACS Appl Mater Interfaces 13(24):28188–28200. https://doi.org/10.1021/acsami.1c05662
10. Chia MY, Thiam HS, Leong LK, Koo CH (2018) Effect of filler content on transport properties of sulfonated polyether ether ketone (SPEEK) composite proton exchange membranes. IOP Conf Ser Mater Sci Eng 409(1):012003. https://doi.org/10.1088/1757-899X/409/1/012003
11. Yang H, Zhang J, Li J, Jiang SP, Forsyth M, Zhu H (2017) Proton transport in hierarchical-structured Nafion membranes: a NMR study. J Phys Chem Lett 8(15):3624–3629. https://doi.org/10.1021/acs.jpclett.7b01557
12. Ng LX, Suhaimin NS, Jaafar J (2022) Polyvinyl alcohol incorporated with mesoporous phosphotungstic acid for direct methanol fuel cell application. J Appl Membr Sci Technol 26(1):1–10. https://doi.org/10.11113/amst.v26n1.227
13. Colpan CO, Ouellette D, Glüsen A, Müller M, Stolten D (2017) Reduction of methanol crossover in a flowing electrolyte-direct methanol fuel cell. Int J Hydrogen Energy 42(33):21530–21545. https://doi.org/10.1016/j.ijhydene.2017.01.004
14. Venkatesan S, Lim C, Rogers E, Holdcroft S, Kjeang E (2015) Evolution of water sorption in catalyst coated membranes subjected to combined chemical and mechanical degradation. Phys Chem Chem Phys 17(21):13872–13881. https://doi.org/10.1039/c5cp01641j
15. Li Z, Hao X, Cheng G, Huang S, Han D, Xiao M, Wang S, Meng Y (2021) In situ implantation of cross-linked functional POSS blocks in Nafion® for high performance direct methanol fuel cells. J Membr Sci 640:119798. https://doi.org/10.1016/j.memsci.2021.119798
16. Yin C, Li J, Zhou Y, Zhang H, Fang P, He C (2018) Enhancement in proton conductivity and thermal stability in Nafion membranes induced by incorporation of sulfonated carbon nanotubes. ACS Appl Mater Interfaces 10(16):14026–14035. https://doi.org/10.1021/acsami.8b01513
17. Wang H, Wen T, Shao Z, Zhao Y, Cui Y, Gao K, Xu W, Hou H (2021) High proton conductivity in Nafion/Ni-MOF composite membranes promoted by ligand exchange under ambient conditions. Inorg Chem 60(14):10492–10501. https://doi.org/10.1021/acs.inorgchem.1c01107
18. Ju J, Shi J, Wang M, Wang L, Cheng B, Yu X, Cai Y, Wang S, Fang L, Kang W (2021) Constructing interconnected nanofibers@ZIF-67 superstructure in nafion membranes for accelerating proton transport and confining methanol permeation. Int J Hydrogen Energy 46(78):38782–38794. https://doi.org/10.1016/j.ijhydene.2021.09.110
19. Guo X, Fan Y, Xu J, Wang L, Zheng J (2020) Amino-MIL-53(Al)-nanosheets@Nafion composite membranes with improved proton/methanol selectivity for passive direct methanol fuel cells. Ind Eng Chem Res 59(33):14825–14833. https://doi.org/10.1021/acs.iecr.0c02741
20. Guo Y, Jiang Z, Wang X, Ying W, Chen D, Liu S, Chen S, Jiang Z, Peng X (2018) Zwitterion threaded metal–organic framework membranes for direct methanol fuel cells. J Mater Chem A 6(40):19547–19554. https://doi.org/10.1039/c8ta08013e
21. Liu Q, Li Z, Wang D, Li Z, Peng X, Liu C, Zheng P (2020) Metal organic frameworks modified proton exchange membranes for fuel cells. Front Chem 8:694. https://doi.org/10.3389/fchem.2020.00694
22. Yin C, Li J, Zhou Y, Zhang H, Fang P, He C (2018) Phase separation and development of proton transport pathways in metal oxide nanoparticle/Nafion composite membranes during water uptake. J Phys Chem C 122(17):9710–9717. https://doi.org/10.1021/acs.jpcc.8b02535
23. Ben Jadi S, El Guerraf A, Bazzaoui EA, Wang R, Martins JI, Bazzaoui M (2019) Synthesis, characterization, and transport properties of Nafion-polypyrrole membrane for direct methanol fuel cell (DMFC) application. J Solid State Electrochem 23(8):2423–2433. https://doi.org/10.1007/s10008-019-04355-w
24. Cai W, Fan K, Li J, Ma L, Xu G, Xu S, Ma L, Cheng H (2016) A bi-functional polymeric nano-sieve Nafion composite membrane: improved performance for direct methanol fuel cell applications. Int J Hydrogen Energy 41(38):17102–17111. https://doi.org/10.1016/j.ijhydene.2016.07.128
25. Dutta K, Das S, Kundu PP (2015) Partially sulfonated polyaniline induced high ion-exchange capacity and selectivity of Nafion membrane for application in direct methanol fuel cells. J Membr Sci 473:94–101. https://doi.org/10.1016/j.memsci.2014.09.010
26. Mollá S, Compañ V (2011) Polyvinyl alcohol nanofiber reinforced Nafion membranes for fuel cell applications. J Membr Sci 372(1–2):191–200. https://doi.org/10.1016/j.memsci.2011.02.001
27. Al-Batty S, Dawson C, Shanmukham SP, Roberts EPL, Holmes SM (2016) Improvement of direct methanol fuel cell performance using a novel mordenite barrier layer. J Mater Chem A 4(28):10850–10857. https://doi.org/10.1039/c6ta03485c

28. Parthiban V, Sahu AK (2020) Performance enhancement of direct methanol fuel cells using a methanol barrier boron nitride–Nafion hybrid membrane. New J Chem 44(18):7338–7349. https://doi.org/10.1039/d0nj00433b
29. Hosseinpour M, Sahoo M, Perez-Page M, Baylis SR, Patel F, Holmes SM (2019) Improving the performance of direct methanol fuel cells by implementing multilayer membranes blended with cellulose nanocrystals. Int J Hydrogen Energy 44(57):30409–30419. https://doi.org/10.1016/j.ijhydene.2019.09.194
30. Rao AS, Rashmi KR, Manjunatha DV, Jayarama A, Veena Devi Shastrimath V, Pinto R (2021) Methanol crossover reduction and power enhancement of methanol fuel cells with polyvinyl alcohol coated Nafion membranes. Mater Today Proc 35:344–351. https://doi.org/10.1016/j.matpr.2020.02.093
31. Lin H-L, Wang S-H (2014) Nafion/poly(vinyl alcohol) nano-fiber composite and Nafion/poly(vinyl alcohol) blend membranes for direct methanol fuel cells. J Membr Sci 452:253–262. https://doi.org/10.1016/j.memsci.2013.09.039
32. Yagizatli Y, Ulas B, Cali A, Sahin A, Ar I (2020) Improved fuel cell properties of nano-TiO2 doped poly(vinylidene fluoride) and phosphonated poly(vinyl alcohol) composite blend membranes for PEM fuel cells. Int J Hydrogen Energy 45(60):35130–35138. https://doi.org/10.1016/j.ijhydene.2020.02.197
33. Ahangar I, Mir FQ (2020) Development of polyvinyl alcohol (PVA) supported zirconium tungstate (ZrW/PVA) composite ion-exchange membrane. Int J Hydrogen Energy 45(56):32433–32441. https://doi.org/10.1016/j.ijhydene.2020.08.216
34. Pandey J, Mir FQ, Shukla A (2014) Synthesis of silica immobilized phosphotungstic acid (Si-PWA)-poly(vinyl alcohol) (PVA) composite ion-exchange membrane for direct methanol fuel cell. Int J Hydrogen Energy 39(17):9473–9481. https://doi.org/10.1016/j.ijhydene.2014.03.237
35. Li Y, Liang L, Liu C, Li Y, Xing W, Sun J (2018) Self-healing proton-exchange membranes composed of Nafion–poly(vinyl alcohol) complexes for durable direct methanol fuel cells. Adv Mater 30(25):1707146. https://doi.org/10.1002/adma.201707146
36. Wu Q, Wang H, Lu S, Xu X, Liang D, Xiang Y (2016) Novel methanol-blocking proton exchange membrane achieved via self-anchoring phosphotungstic acid into chitosan membrane with submicro-pores. J Membr Sci 500:203–210. https://doi.org/10.1016/j.memsci.2015.11.019
37. Pourzare K, Mansourpanah Y, Farhadi S, Sadrabadi MMH, Ulbricht M (2022) Improvement of proton conductivity of magnetically aligned phosphotungstic acid-decorated cobalt oxide embedded Nafion membrane. Energy 239:121940. https://doi.org/10.1016/j.energy.2021.121940
38. Abouzari-Lotf E, Nasef MM, Ghassemi H, Zakeri M, Ahmad A, Abdollahi Y (2015) Improved methanol barrier property of Nafion hybrid membrane by incorporating nanofibrous interlayer self-immobilized with high level of phosphotungstic acid. ACS Appl Mater Interfaces 7(31):17008–17015. https://doi.org/10.1021/acsami.5b02268
39. Parthiban V, Akula S, Peera SG, Islam N, Sahu AK (2016) Proton conducting nafion-sulfonated graphene hybrid membranes for direct methanol fuel cells with reduced methanol crossover. Energy Fuels 30(1):725–734. https://doi.org/10.1021/acs.energyfuels.5b02194
40. Changkhamchom S, Sirivat A (2019) Sulfonated (graphene oxide/poly(ether ketone ether sulfone) (S-GO/S-PEKES) composite proton exchange membrane with high proton conductivity for direct methanol fuel cell. Polym-Plast Technol Mater 58(17):1900–1913. https://doi.org/10.1080/25740881.2019.1587770
41. Shabanpanah S, Omrani A, Mansour Lakouraj M (2019) Fabrication and characterization of PVA/NNSA/GLA/nano-silica proton conducting composite membranes for DMFC applications. Des Monomers Polym 22(1):130–139. https://doi.org/10.1080/15685551.2019.1626323
42. Di Virgilio M, Basso Peressut A, Arosio V, Arrigoni A, Latorrata S, Dotelli G (2023) Functional and environmental performances of novel electrolytic membranes for PEM fuel cells: a lab-scale case study. Clean Technologies 5(1):74–93. https://doi.org/10.3390/cleantechnol5010005
43. Ma L, Li J, Xiong J, Xu G, Liu Z, Cai W (2017) Proton conductive channel optimization in methanol resistive hybrid hyperbranched polyamide proton exchange membrane. Polymers 9(12):703. https://doi.org/10.3390/polym9120703
44. Sigwadi R, Dhlamini MS, Mokrani T, Nemavhola F, Nonjola PF, Msomi PF (2019) The proton conductivity and mechanical properties of Nafion(R)/ ZrP nanocomposite membrane. Heliyon 5(8):e02240. https://doi.org/10.1016/j.heliyon.2019.e02240
45. Imaan DU, Mir FQ, Ahmad B (2021) Synthesis and characterization of a novel poly (vinyl alcohol)-based zinc oxide (PVA-ZnO) composite proton exchange membrane for DMFC. Int J Hydrogen Energy 46(22):12230–12241. https://doi.org/10.1016/j.ijhydene.2020.05.008
46. Lee S-H, Choi S-H, Gopalan S-A, Lee K-P, Anantha-Iyengar G (2014) Preparation of new self-humidifying composite membrane by incorporating graphene and phosphotungstic acid into sulfonated poly(ether ether ketone) film. Int J Hydrogen Energy 39(30):17162–17177. https://doi.org/10.1016/j.ijhydene.2014.07.181
47. Zhou Y, Yang J, Su H, Zeng J, Jiang SP, Goddard WA (2014) Insight into proton transfer in phosphotungstic acid functionalized mesoporous silica-based proton exchange membrane fuel cells. J Am Chem Soc 136(13):4954–4964. https://doi.org/10.1021/ja411268q
48. Kim Y, Ketpang K, Jaritphun S, Park JS, Shanmugam S (2015) A polyoxometalate coupled graphene oxide–Nafion composite membrane for fuel cells operating at low relative humidity. J Mater Chem A 3(15):8148–8155. https://doi.org/10.1039/c5ta00182j
49. Pourzare K, Farhadi S, Mansourpanah Y (2018) Anchoring $H_3PW_{12}O_{40}$ on aminopropylsilanized spinel-type cobalt oxide (Co_3O_4-$SiPrNH_2$/$H_3PW_{12}O_{40}$): a novel nanohybrid adsorbent for removing cationic organic dye pollutants from aqueous solutions. Appl Organomet Chem 32(5):e4341. https://doi.org/10.1002/aoc.4341
50. Meng X, Song K, Lv Y, Cong C, Ye H, Dong Y, Zhou Q (2021) SPEEK proton exchange membrane with enhanced proton conductivity stability from phosphotungstic acid-encapsulated silica nanorods. Mater Chem Phys 272:125045. https://doi.org/10.1016/j.matchemphys.2021.125045
51. Priyangga A, Atmaja L, Santoso M, Jaafar J, Ilbeygi H (2022) Utilization of mesoporous phosphotungstic acid in nanocellulose membranes for direct methanol fuel cells. RSC Adv 12(23):14411–14421. https://doi.org/10.1039/d2ra01451c
52. Rao US, Sekharnath K, Sudhakar H, Rao KC, Subha M (2014) Mixed matrix membranes of sodium alginate and hydroxy propyl cellulose loaded with phosphotungstic heteropolyacid for the pervaporation separation of water–isopropanol mixtures At 30 0 C. Int J Sci Technol Res 3:129–137
53. Härk E, Jäger R, Tallo I, Joost U, Möller P, Romann T, Kanarbik R, Steinberg V, Kirsimäe K, Lust E (2017) Influence of chemical composition and amount of intermixed ionomer in the catalyst on the oxygen reduction reaction characteristics. J Solid State Electrochem 21(7):2079–2090. https://doi.org/10.1007/s10008-017-3521-7
54. Kim DS, Cho HI, Kim DH, Lee BS, Lee BS, Yoon SW, Kim SY, Moon GY, Byun HS, Rhim JW (2009) Surface fluorinated poly(vinyl alcohol)/poly(styrene sulfonic acid-co-maleic acid) membrane for polymer electrolyte membrane fuel cells. J Membr Sci 342:138–144. https://doi.org/10.1016/j.memsci.2009.06.034
55. Ben Jadi S, El Guerraf A, Kiss A, El Azrak A, Bazzaoui EA, Wang R, Martins JI, Bazzaoui M (2020) Analyses of scanning electrochemical microscopy and electrochemical impedance spectroscopy in direct methanol fuel cells: permeability resistance and proton conductivity of polyaniline modified membrane. J Solid State Electrochem 24(7):1551–1565. https://doi.org/10.1007/s10008-020-04659-2

56. Xu J, Zhang Q, Cheng Y-T (2016) High capacity silicon electrodes with Nafion as binders for lithium-ion batteries. J Electrochem Soc 163:A401–A405. https://doi.org/10.1149/2.0261603jes
57. Friedman AK, Shi W, Losovyj Y, Siedle AR, Baker LA (2018) Mapping microscale chemical heterogeneity in Nafion membranes with X-ray photoelectron spectroscopy. J Electrochem Soc 165(11):H733. https://doi.org/10.1149/2.0771811jes
58. Li Y, Fang X, Wang Y, Ma B, Sun J (2016) Highly transparent and water-enabled healable antifogging and frost-resisting films based on poly(vinyl alcohol)–Nafion complexes. Chem Mater 28(19):6975–6984. https://doi.org/10.1021/acs.chemmater.6b02684
59. Lu S, Xu X, Zhang J, Peng S, Liang D, Wang H, Xiang Y (2014) A self-anchored phosphotungstic acid hybrid proton exchange membrane achieved via one-step synthesis. Adv Energy Mater 4(17):1400842. https://doi.org/10.1002/aenm.201400842
60. Shi W, Li H, Zhou R, Qin X, Zhang H, Su Y, Du Q (2016) Preparation and characterization of phosphotungstic acid/PVA nanofiber composite catalytic membranes via electrospinning for biodiesel production. Fuel 180:759–766. https://doi.org/10.1016/j.fuel.2016.04.066
61. Huang H, Ma Y, Jiang Z, Jiang Z-J (2021) Spindle-like MOFs-derived porous carbon filled sulfonated poly (ether ether ketone): a high performance proton exchange membrane for direct methanol fuel cells. J Membr Sci 636:119585. https://doi.org/10.1016/j.memsci.2021.119585
62. Akbari S, Mosavian MTH, Ahmadpour A, Moosavi F (2017) Water dynamics and proton-transport mechanisms of Nafion 117/phosphotungstic acid composite membrane: a molecular dynamics study. ChemPhysChem 18(23):3485–3497. https://doi.org/10.1002/cphc.201700725
63. Mohanapriya S, Bhat SD, Sahu AK, Pitchumani S, Sridhar P, Shukla AK (2009) A new mixed-matrix membrane for DMFCs. Energy Environ Sci 2(11):1210. https://doi.org/10.1039/b909451b
64. Hamid NSA, Kamarudin SK, Karim NA (2021) Potential of Nafion/eggshell composite membrane for application in direct methanol fuel cell. Int J Energy Res 45(2):2245–2264. https://doi.org/10.1002/er.5917
65. Abu-Saied MA, Soliman EA, Abualnaj KM, El Desouky E (2021) Highly conductive polyelectrolyte membranes poly(vinyl alcohol)/poly(2-acrylamido-2-methyl propane sulfonic acid) (PVA/PAMPS) for fuel cell application. Polymers 13(16):2638. https://doi.org/10.3390/polym13162638
66. Kim AR, Park CJ, Vinothkannan M, Yoo DJ (2018) Sulfonated poly ether sulfone/heteropoly acid composite membranes as electrolytes for the improved power generation of proton exchange membrane fuel cells. Compos B Eng 155:272–281. https://doi.org/10.1016/j.compositesb.2018.08.016
67. Kulasekaran P, Maria Mahimai B, Deivanayagam P (2020) Novel cross-linked poly(vinyl alcohol)-based electrolyte membranes for fuel cell applications. RSC Adv 10(44):26521–26527. https://doi.org/10.1039/d0ra04360e
68. Fan C, Wu H, Li Y, Shi B, He X, Qiu M, Mao X, Jiang Z (2020) Incorporating self-anchored phosphotungstic acid@triazole-functionalized covalent organic framework into sulfonated poly(ether ether ketone) for enhanced proton conductivity. Solid State Ionics 349:115316. https://doi.org/10.1016/j.ssi.2020.115316
69. Xu L, Han H, Liu M, Xu J, Ni H, Zhang H, Xu D, Wang Z (2015) Phosphotungstic acid embedded sulfonated poly(arylene ether ketone sulfone) copolymers with amino groups for proton exchange membranes. RSC Adv 5(101):83320–83330. https://doi.org/10.1039/c5ra13115d
70. Tersulfon O-PEK (2017) Methanol permeability and properties of polymer electrolyte membrane based on graphene oxide-sulfonated (polyether ether) ketone. Malaysian J Anal Sci 21(2):435–444. https://doi.org/10.17576/mjas-2017-2102-19
71. Uma Devi A, Divya K, Rana D, Sri Abirami Saraswathi M, Nagendran A (2018) Highly selective and methanol resistant polypyrrole laminated SPVdF-co-HFP/PWA proton exchange membranes for DMFC applications. Mater Chem Phys 212:533–542. https://doi.org/10.1016/j.matchemphys.2018.03.086
72. Zhang H, Xia H, Zhao Y (2012) Poly(vinyl alcohol) hydrogel can autonomously self-heal. ACS Macro Lett 1(11):1233–1236. https://doi.org/10.1021/mz300451r
73. Chen C-Y, Garnica-Rodriguez JI, Duke MC, Costa RFD, Dicks AL, da Costa JCD (2007) Nafion/polyaniline/silica composite membranes for direct methanol fuel cell application. J Power Sources 166(2):324–330. https://doi.org/10.1016/j.jpowsour.2006.12.102
74. Tang Y, Yuan W, Pan M, Tang B, Li Z, Wan Z (2010) Effects of structural aspects on the performance of a passive air-breathing direct methanol fuel cell. J Power Sources 195(17):5628–5636. https://doi.org/10.1016/j.jpowsour.2010.03.069
75. Prapainainar P, Du Z, Kongkachuichay P, Holmes SM, Prapainainar C (2017) Mordenite/Nafion and analcime/Nafion composite membranes prepared by spray method for improved direct methanol fuel cell performance. Appl Surf Sci 421:24–41. https://doi.org/10.1016/j.apsusc.2017.02.004
76. Hashim N, Kamarudin SK, Daud WRW (2009) Design, fabrication and testing of a PMMA-based passive single-cell and a multi-cell stack micro-DMFC. Int J Hydrogen Energy 34(19):8263–8269. https://doi.org/10.1016/j.ijhydene.2009.07.043
77. Abdullah N, Kamarudin SK, Shyuan LK (2018) Novel anodic catalyst support for direct methanol fuel cell: characterizations and single-cell performances. Nanoscale Res Lett 13(1):90. https://doi.org/10.1186/s11671-018-2498-1
78. Kamitani A, Morishita S, Kotaki H, Arscott S (2008) Miniaturized microDMFC using silicon microsystems techniques: performances at low fuel flow rates. J Micromech Microeng 18(12):125019. https://doi.org/10.1088/0960-1317/18/12/125019